Experiments in Fluids 14, 233–240 (1993)

Experiments in Fluids

A new laser based technique for instability growth rate evaluation in liquid jets

G. E. Cossali and **A. Coghe**

Politecnico di Milano, Dipartimento di Energetica, Piazza L. da Vinci n. 32, 20133 Milan – Italy

1 Introduction

Rayleigh instability of a liquid jet has been extensively studied during the past century and a theoretical solution for the inviscid case was published in 1875 by Rayleigh. Extensions of the solution were proposed by Weber (1931), Levich (1962), Levich and Krylov (1969) and Sleicher (1975), the full linear viscous theory was given by Chandrasekhar. Nonlinear theory has also been used to deal with the problem, a classical paper being that of Bohr (1909); more recent work is that of Wang (1968) and Yuen (1968). Experimental tests of those solutions have been reported and the most comprehensive analysis seems to be that of Donnelly and Glaberson which made use of a photographic technique in order to evaluate the instability growth rate as a function of wave number. More recently other results, making use of a similar technique, have been reported (Sakai et al. 1985).

Photographic techniques are quite time-consuming: evaluation of growth rate by direct measurement of the pictures is not always easy and the procedure must be repeated for all the wave numbers of interest. The technique proposed here allows the growth rate to be evaluated for any wave number by a direct Fourier transform of the signal output from a photodiode on which a laser beam of low power, crossing the liquid jet, has been imaged. The advantage of this technique relies on the rapidity of the procedure and the simple setup needed, whereas the uncercainty does not seem to be greater than that obtained using the conventional technique.

2 Basic principles

The idea of the technique is to relate the deflection of a laser beam passing through a liquid jet to the variation of the liquid column radius. Thus the spectrum of the surface perturbation can be obtained from the detection of the beam deflection as a function of time. By comparison of the spectra obtained at different distances from the nozzle exit i.e. at different times after the surface perturbation began, the growth rate of any Fourier component is obtained.

Let us first consider the following ideal experiment: a laser beam passes through a cylindrical liquid column which acts as a cylindrical lens spreading the light into a sheet normal to the cylinder axis. Since the optical path of the light beam passing through the cylinder diameter is unperturbed, if a photosensitive element is positioned as in Fig. 1 a then it will collect light coming from the region x_1 of the laser beam. If the column shape is changed by a sinusoidal perturbation (Fig. 1 b) the surface equation will become: $r = R + \delta \sin(k x)$ (where R is the unperturbed jet radius, and k the wave number of the perturbation). Due to refraction, the light falling onto the photosensitive element will now emerge from a different region (x_2 in Fig. 1 b) and, due to the nonuniform light distribution inside the laser beam, that will produce a variation of the photodetector output signal. Let us assume that the liquid column is moving as a whole along the z direction with velocity V. At different times the light falling onto the photodetector will come from a different region (x_3) of the light beam (Fig. 1 c) and the photodetector signal output will vary periodically with time. Such variation will be characterized by a period that is related to the wave number of the surface perturbation by the relation: $T = 2\pi/kV$ and observation of the output signal will readily yield the perturbation wave number.

It must be pointed out that the assumed one-to-one correspondence between received intensity and position in the beam is acceptable only if the wavelength of the perturbation is greater then the width of the light beam, otherwise two or more different parts of the light beam may be brought to overlap at the detection location. If the perturbation is not sinusoidal and there is an interest in identifying the spectrum of the perturbation in the signal output, more detailed analysis is required.

Laser beam deflection can be studied with sufficient precision by geometrical optics, and Snell's law applied to the model shown in Fig. 2 gives the following equations:

$$\frac{\sin(\Theta)}{\sin(\Theta - \Omega)} = m_{12} \tag{1}$$

$$\frac{\sin(\phi + \beta)}{\sin(\Omega + \beta)} = m_{12} \tag{2}$$

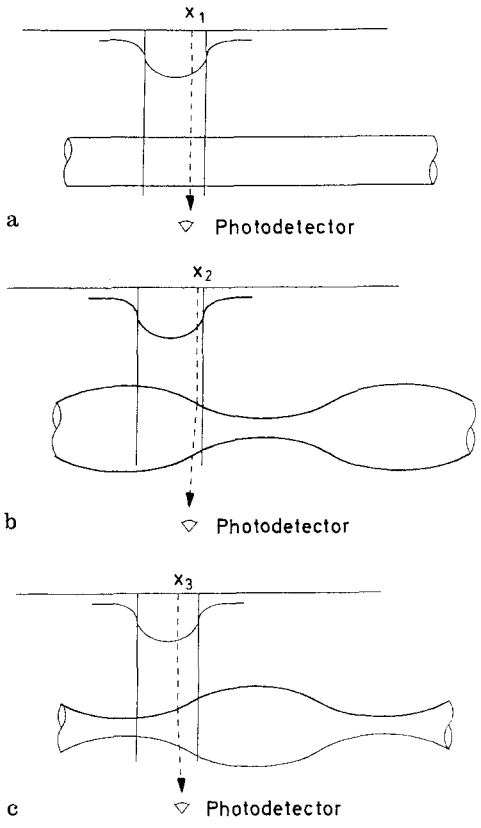

Fig. 1 a–c. Optical path through unperturbed and perturbed liquid column

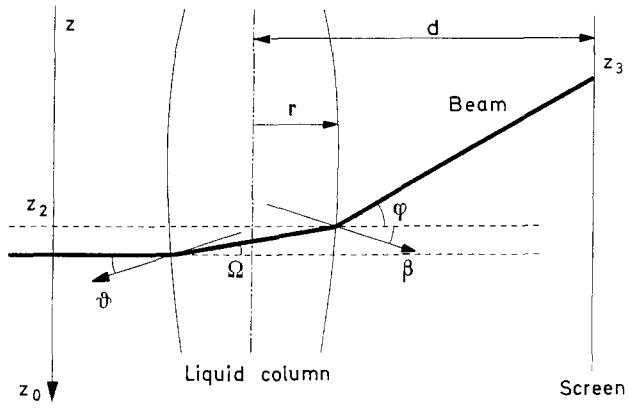

Fig. 2. Light beam deflection through radially symmetric liquid column

where m_{12} is the relative refractive index. Always referring to Fig. 2, the angles Θ and β can be defined by means of the derivative of the function $r(z)$ (the radius of the liquid column) at the points where the light beam crosses the surface:

$$\sin(\Theta) = \frac{r'(z_0)}{[1+r'(z_0)^2]^{1/2}} \tag{3}$$

$$\sin(\beta) = \frac{r'(z_2)}{[1+r'(z_2)^2]^{1/2}} \tag{4}$$

where $r'(z) = dr(z)/dz$. The z-coordinate where the light beam crosses the two interfaces and reaches the screen, located at a distance "d" from the jet axis, may be related geometrically through the expressions:

$$z_2 = z_0 + \tan(\Omega) \cdot [r(z_2) + r(z_0)] \tag{5}$$

$$z_3 = z_2 + [d - r(z_2)] \cdot \tan(\phi). \tag{6}$$

Equation (1)–(6) contain six unknowns (z_2, z_3, Ω, ϕ, β, Θ) if one supposes that the liquid column shape is known and z_0 is given; the beam displacement $(z_3 - z_0)$ can then be obtained as a function of the position where the beam crosses the first interface (z_0). For an analytical solution, Eqs. (1)–(6) must be linearized and that is possible provided:

$$r'(z_0) \ll 1 \quad \text{and} \quad r''(z_0) \cdot r(z_0) \ll 1 \tag{7}$$

which is acceptable when the perturbation amplitude is small, i.e. for z_0 not too close to the break-up region. By using Eq. (3) and (4) to eliminate Θ and β from Eq. (1) and (2), and using Eq. (7) to obtain:

$$r(z_2) = r(z_0) + r'(z_0) \cdot (z_2 - z_0) + o(z_2 - z_0)$$

and

$$r(z_2) + r(z_0) = 2r(z_0) + r'(z_0) \cdot (z_2 - z_0) + o(z_2 - z_0).$$

Eqs. (1)–(6) can be transformed into a set of four linear equations (neglecting the terms of higher order than one, symbolized by $o(z_2 - z_0)$):

$$\Omega = \frac{m_{12}-1}{m_{12}} r' \tag{8a}$$

$$z_2 - z_0 = 2\frac{m_{12}-1}{m_{12}} r' r \tag{8b}$$

$$\phi = 2(m_{12}-1) r' \tag{8c}$$

$$z_3 = z_0 + 2\frac{m_{12}-1}{m_{12}} r' r + [d - r + r' \cdot (z_2 - z_0)] \cdot \phi \tag{8d}$$

where $r' = r'(z_0)$ and $r'(z_2) = r'(z_0) + r''(z_0)(z_2 - z_0) + \ldots$ so that $r'(z_2) = r'$ with the accuracy accepted here. The solution of Eq. (8a–d) can be easily obtained by substitution, yielding:

$$z_3 - z_0 = 2(m_{12}-1) r' \left[d - \frac{m_{12}-1}{m_{12}} r \right] = D \cdot r'. \tag{9}$$

Equation (9) gives the value of z_3 when z_0 and the column shape are known; it is important to be able to calculate explicitly the value $z_3 - z_0$ when z_3 is given and this is possible from Eq. (9) if the following conditions are satisfied (see Appendix):

$$d \gg r \quad \text{and} \quad |r'' \cdot D| \ll 1. \tag{10}$$

If (10) is valid, $r'(z_0)$ can be substituted by $r'(z_3)$ obtaining:

$$z_3 - z_0 = D r' \tag{11}$$

where D may be considered a constant and now $r' = r'(z_3)$. The light falling onto the photosensitive element positioned at z_3 is that coming from position z_0 and if the light intensity of the laser beam is linearly distributed around position z_3, i.e.

$$I_i(z) = \alpha \cdot (z - z_3) + I_0$$

then the light intensity falling onto the photosensitive element located at z_3 (neglecting variation in absorption and reflection, due to small variations in angles of incidence and then in optical paths) becomes:

$$I_c(z_3) = I_i(z_0) = \alpha \cdot (z_0 - z_3) + I_0 = I_0 - \alpha \cdot D \cdot r' \tag{12}$$

and I_c is then proportional to r' except for the constant I_0 which will produce a DC component on the photosensor's output signal, which can easily be eliminated by electronic means. Equations (12) holds as long as the hypothesis of linear light distribution is maintained, i.e. with any light intensity distribution if $(z_0 - z_3)$ is sufficiently small. A discussion of this point will be provided in the next section, but it must be said that $z_0 - z_3$ depends on the liquid column perturbation amplitude; thus the linearity condition is satisfied if the observed jet location is far enough from the break-up region.

Let us consider an infinite liquid column whose radius at each location z and time t_1 is given by the function: $r(z, t_1)$ which may be defined using its Fourier transform:

$$r(z, t_1) = \int \Gamma(k, t_1)\, e^{ikz}\, dk. \tag{13}$$

The evolution of the perturbation is governed by the following equation (Rayleigh, 1875):

$$\Gamma(k, t_2) = \Gamma(k, t_1)\, e^{s(k) \cdot (t_2 - t_1)} \tag{14}$$

where $s(k)$ is the instability growth rate. By defining a new variable as: $\tau = z/V$, where V is a constant, one may write:

$$r(z, t) = r(V\tau, t) = r_v(\tau, t)$$

and

$$r_v(\tau, t) = \int \Gamma_v(w, t)\, e^{iw\tau}\, dw \tag{13'}$$

where $w = kV$ and $\Gamma_v(w, t) = \dfrac{\Gamma(w/V, t)}{V}$

and defining: $p(w) = s(w/V)$ Eq. (14) becomes:

$$\Gamma_v(w, t_2) = \Gamma_v(w, t_1)\, e^{p(w) \cdot (t_2 - t_1)}. \tag{14'}$$

In the real case the jet is observed at a point whose distance from the nozzle exit is x_1 and the jet radius there is $r(\tau)$ at time τ. If V is the jet velocity $t_1 = x_1/V$ is the time needed by the fluid particle to travel from the nozzle exit to the observation point; thus $r_{x_1}(\tau)$ may be considered as the value of the jet radius at a time t_1 of its evolution at any spatial location (defined by τ and V) along the jet axis [as though a jet of infinite length frozen at a time t_1 of its evolution was travelling at a velocity V and its radius observed at a fixed location]. By observing the actual jet at different distances from the nozzle, different stages of the instability evolution will be seen and it is clear that:

$$r_{x_1}(\tau) = r_v(\tau, t_1) \quad \text{where} \quad t_1 = x_1/V.$$

If the photosensitive element produces a signal output proportional to the light intensity falling upon it, the DC part of such a signal can be extracted and the result is proportional to r':

$$U_{x_1}(\tau) = C \cdot r'_v(\tau, t_1)/V \quad \text{where} \quad r'_v(\tau, t) = \frac{dr_v(\tau, t)}{d\tau}.$$

Thus, the Fourier transform of $U(\tau)$ is:

$$G(w, t_1) = \frac{1}{2\pi} \int U_{x_1}(\tau)\, e^{-iw\tau}\, d\tau$$

$$= \frac{iwC}{2\pi V} \int r_v(\tau, t_1)\, d\tau = \frac{iwC}{2\pi V}\, \Gamma_v(w, t_1) \tag{15}$$

and changing the observation point to x_2, the Fourier transform of the output signal becomes:

$$G(w, t_2) = \frac{iwC}{2\pi V}\, \Gamma_v(w, t_2)$$

and by using (14') and (15) one obtains:

$$|G(w, t_2)| = |G(w, t_1)|\, e^{p(w) \cdot (t_2 - t_1)}$$

or

$$p(w) = \frac{1}{(t_2 - t_1)} \log \left[\frac{|G(w, t_2)|}{|G(w, t_1)|} \right] \tag{16}$$

showing that the growth rate $s(k) = p(kV)$ can be calculated by the spectrum of the photodetector output signal obtained at two different locations (x_1, x_2) and the jet velocity (V).

3 Numerical assessment of the technique

A numerical simulation of the technique explained above has been performed in order to analyze the effect of some parameters on the accuracy of the final results. A Gaussian distribution of the light intensity, as found in a laser beam (TEM_{00}), was considered because this light source appears to be the most suitable for such an experiment, in terms of beam parallelism, light intensity and time stability.

The simulation programme was able to yield the photodiode output when any perturbation of the liquid column was given, by solving Eqs. (1)–(6) numerically. The photodetector was considered perfect, with zero delay time and no electronic noise; that was done because the purpose of the present simulation was mainly to study the effect of the parameters such as screen distance from the jet, beam–photodetector relative position, and perturbation amplitude on the validity of the linearization hypothesis and then on the overall accuracy of the technique, and the introduction of photodetector characteristics was considered uninteresting at this stage.

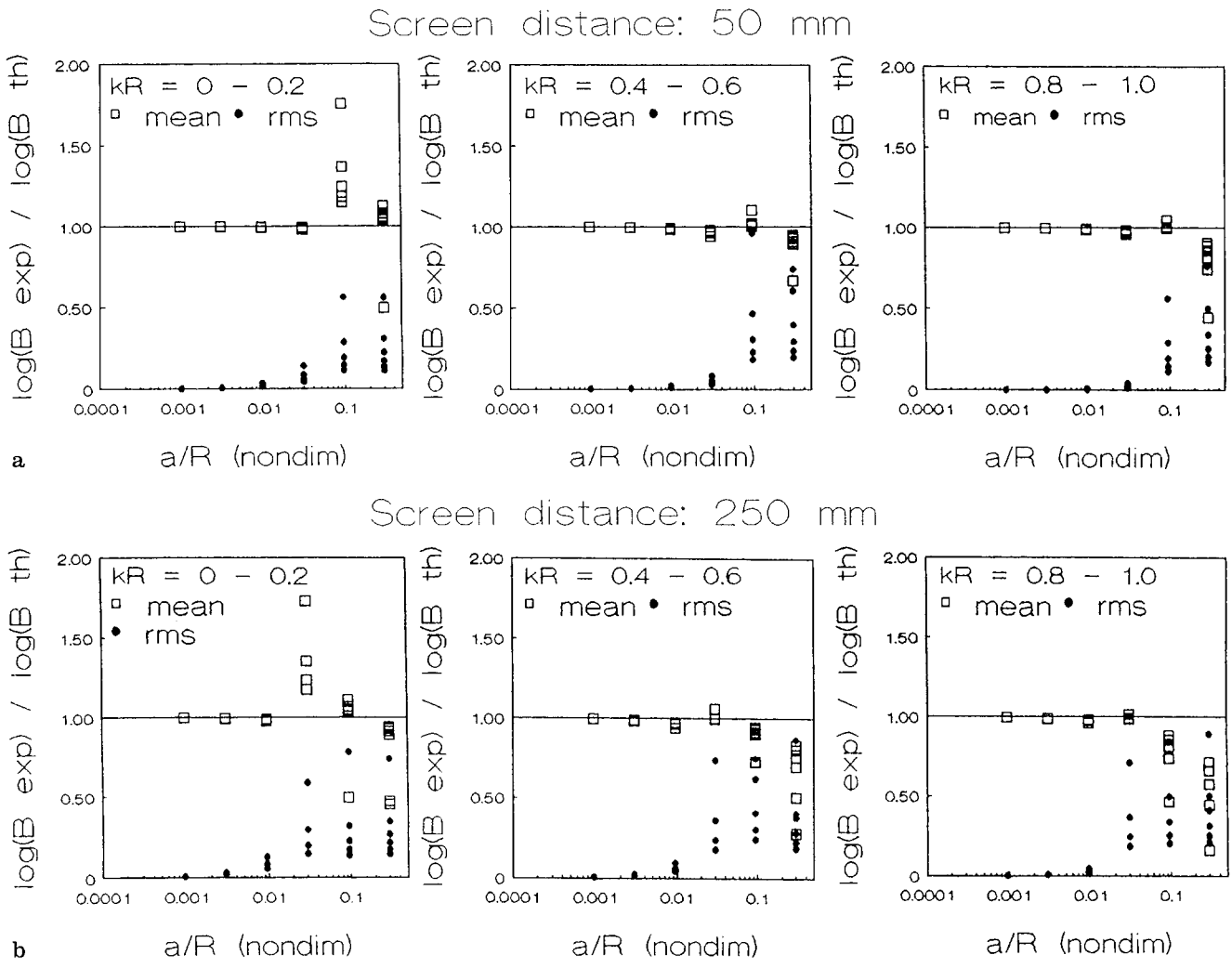

Fig. 3. a Fourier component intensity ratio vs. disturbance amplitude; screen distance from jet: 50 mm. **b** Fourier component intensity ratio vs. disturbance amplitude; screen distance from jet: 250 mm

The liquid column shape is provided by the function $r(x)$ that for the present simulation was obtained by superimposing 20 harmonic functions, with wave numbers uniformly distributed over the allowed range (0 to $1/R$) and with the same amplitude "a". If the function $r(x)$ is the input, the simulation provides the Fourier transform of the photodetector output signal.

Because of the fact that the technique is expected to give the distribution, within the allowed range of wave numbers, of the ratio between Fourier component intensity measured at different distances from the nozzle, thus having different amplitudes, the output spectra for input functions having different disturbance amplitude were used to generate those ratios and the results compared with the expected value of such ratios, as a function of wave number and disturbance amplitude. The simulation was repeated for different values of screen distance "d".

In Figs. 3a–b, B is the average value (over a defined range of wave numbers) of the Fourier component intensity ratio obtained by two simulations relative to the input function $r(x)$ having different disturbance amplitudes "a", i.e. $B_{exp} = |G_2(w)|/|G_1(w)|$ where $|G_j(w)|$ is the Fourier component intensity relative to the input function $r(x)$ having disturbance amplitude equal to a_j. Then B_{exp} is expected to have a value equal to the disturbance amplitude ratio ($B_{th} = a_2/a_1$) and deviations from this value are reported in logarithmic form. The graphs show that increasing the disturbance amplitude does not affect the results if the amplitude remains under 0.01 times the jet radius, but a sharp increase in the spectra variability and errors are noticed when "a" is increased above this value, although the threshold value increases when the photodetector–jet distance is decreased (the abscissa in Figs. 3a–b is the larger amplitude of the two signals used to generate the ratios B, nondimensionalized by the jet radius).

As pointed out in the Appendix, the group $D \cdot a/R^2$ is important to evaluate the correctness of the introduced linearization, and such a group comes close to one for the

imposed values of photodetector distance, jet radius and disturbance amplitude near the obtained threshold levels. Such values of the disturbance amplitude are expected only quite close to the break-up region, but it should be stressed that higher values of disturbance amplitude produce better signal-to-noise ratios, due to the fact that a higher perturbation amplitude produces higher deflection angles, so light coming from a larger laser beam region would reach the photodetector, resulting in a larger amplitude of the A.C. signal output. Better results are then obtained, compromising the opposing requirements of validity of linearization and acceptable signal-to-noise ratio.

4 Effects of finite size of the photodetector

The results obtained above hold for a point-like photosensitive element, but from a practical point of view such an object is neither realizable nor easy to approximate by existing photodiodes. Let us suppose that the minimum perturbation wavelength is much larger than the laser beam diameter, then the function $r'(z_0)$ in Eq. (9) is, to a first approximation, constant when z_0 spans the beam diameter.

The light intensity distribution at the distance "d" from the jet is then shifted by a length $D \cdot r'$ relative to the distribution at the jet location (see Eq. (9)), and the effect of the perturbation of the liquid column on the photodiode output is identical to a displacement of magnitude $D\,r'$ of the photodiode from its normal position when the liquid column is left unperturbed.

Let $R(x)$ be the photodiode output when the liquid column is unperturbed and the photodiode is displaced by the length "x" from its normal position, then $R(0)$ is the output when the photodiode is not displaced and $R(Dr')$ is the output when the photodiode is not displaced and the liquid column is perturbed.

Defining

$$\alpha(x) = \frac{R(x) - R(0)}{x} \tag{17}$$

then $R(x) = R(0) + \alpha \cdot x$ and the photodiode output is linear in x as long as α is constant, and in this case the results obtained from Eq. (12) are still valid. Thus finiteness of the photosensitive element does not negatively affect the technique performance as long as the above-mentioned conditions are satisfied.

5 Experimental configuration

Figure 4 shows the experimental setup: a large tank, containing water, was connected through a pipe to the nozzle holder on which different types of nozzle or needle can be mounted; the nozzle holder can be translated along the vertical direction and it was provided with a system for checking the correct alignment of the nozzles. A level indicator

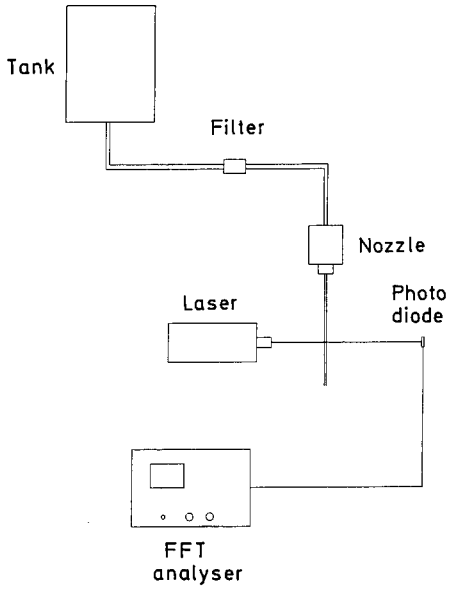

Fig. 4. Experimental setup and measurement system

was connected to the tank and a filter was mounted on the feeding line.

The measurement system comprised a small He-Ne laser (5 mW) and a photodiode, mounted on a micrometer translator, whose output after amplification was sent to a FFT analyser. Data, in the form of signal spectra, were then stored on floppy disk and subsequently reduced by the use of a microcomputer. The correct alignment of the measurement system requires the photodiode to be positioned to get the maximum value of the function $\alpha(x)$ in Eq. (17). The alignment procedure comprised two main steps:

1) positioning the photodetector to receive the light from any region lying on the vertical symmetry axis of the laser beam cross section, and that could be obtained by maximizing the photodiode, D.C. signal output by moving the photodiode along the horizontal direction; 2) moving the photodetector along the vertical direction in order to reach the required position where $\alpha(x)$ is a maximum, and that was obtained by maximizing the D.C. output intensity difference from two subsequent equispaced photodiode locations.

Figure 5 shows the function $\alpha(x)$ measured for the photodiode used for the present experiments, and it can be seen that if $Dr' < 0.1$ mm then α varies less then 5%. The laser beam was evaluated to be 0.84 mm at the jet location; from the Rayleigh theory of the instability, the smallest wave number of a growing perturbation is $2\pi R$, then the present beam width, which is comparable with the liquid column diameter used for the experiments (see below), is still acceptable in order to avoid overlapping of light coming from different beam regions. But it can be questionable for the linearization hypothesis mentioned in the previous paragraph, and relevant errors must be expected at wave numbers close to the maximum value.

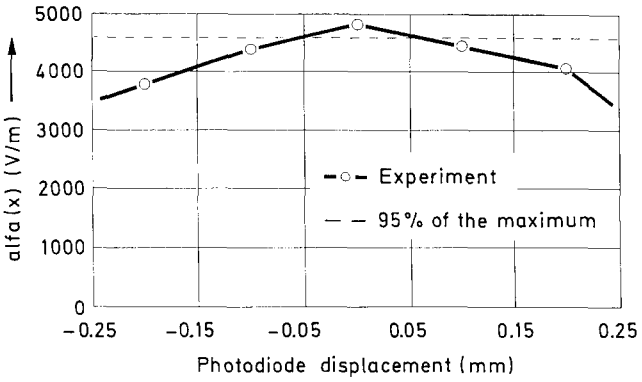

Fig. 5. Values of α for the present experiment

The jet diameter was measured by photographing the jet close to a micrometer and making a direct comparison after enlarging the picture; the accuracy was estimated to be better than 3%.

Jet velocity is an important input value for the calculation procedure and it was measured by a volumetric method, once the jet diameter was known. The distance of the laser beam from the nozzle exit was measured with 0.5 mm error, but relative measurement locations, the only ones important in defining the difference (t_2-t_1) in Eq. (16), were defined with 0.01 mm error; the effect of gravity, although very small, was taken into account by calculating (t_2-t_1) from measurement locations and jet velocity.

Two hole-nozzles of different diameter (0.5 mm and 1.0 mm) and two hypodermic needles (0.5 mm and 0.9 mm) were used, while the jet velocity varied between 1 m/s and 3 m/s, in order to maintain the flow in the laminar regime where Rayleigh instability takes place. The measurement procedure consisted in positioning the light beam at different distances from the nozzle and collecting the photodiode output signal spectra. Subsequently, from the knowledge of the relative position and jet velocity, the growth rate was evaluated by numerically implementing the above explained method.

6 Discussion of the results

The proposed technique has been tested by applying it to the analysis of the liquid jet instability under different experimental conditions and the results, in the form of a growth rate function, were compared with those predicted by the theory Chandrasekhar (1961). Table 1 shows the different conditions under which the technique has been tested. The photodiode signal output was fed to an FFT analyser and 64 spectra, calculated over 1024 points, were accumulated (64 being the maximum number allowed by the instrument) in order to reduce the variability. The result was then transferred to a microcomputer for subsequent data analysis. For each experimental condition of Table 1, measurement of the output spectrum was done by positioning the laser beam at

Table 1. Experimental conditions analysed; cases giving inconsistent results are marked with ×

Velocity (m/s)	Nozzle ($R=$ 0.25 mm)	Nozzle ($R=$ 0.5 mm)	Needle ($R=$ 0.25 mm)	Needle ($R=$ 0.45 mm)
3.00	×			
2.75	o			
2.50	o			
2.35	o		o	
2.25	o			×
2.15	o	×		o
1.95	o	o		
1.85	o	o		
1.75	o	×	o	
1.60	o		o	o
1.50	o		o	o
1.35	o			o
1.25			o	
1.20	o		o	o
1.00	×		o	o

different distances from the nozzle, from the nozzle exit to the break-up region, and the spectral comparison of measurements obtained at different distances allowed the evaluation of the dispersion function. Spectra obtained too close to the break-up region showed great distortion, probably due to the fact that the linear approximation leading to equation (16) is not longer valid when the perturbation amplitude becomes too high (as already observed in the previous paragraphs). The spectral intensity of the signals obtained too close to the nozzle are too low compared with the statistical variability; moreover spectra obtained at positions too close to each other are not sufficiently different to provide detectable information about the perturbation evolution.

Better results have been obtained for any spectrum pair at locations not closer than 5 mm to each other. However, the optimum proximity of the measurement location pair depends on the jet velocity, and the minimum value is also imposed by the measurement accuracy of the distance between locations, which influences the accuracy of the value t_1-t_2 in Eq. (16). Consistency of the results was checked by measuring at n different locations and calculating the dispersion function by comparison of the $n-1$ independent pairs of spectra. In the present case, 5 mm equally spaced measurement locations were used and a comparison scheme as shown in Fig. 6 was used. Rejection of erroneous results due to the effects previously explained was performed by visual comparison.

Figure 7 shows the comparison with Chandrasekhar's (1961) solution for different jet velocities and different nozzle diameters. Results appear to reproduce the predictions satisfactorily, except for very small values of the wave number, and for values close to the maximum allowed ($k_{max}=1/R$). Such discrepancies may be explained by the fact that the spectral magnitude usually has low values for wave numbers close to $1/R$, the short wavelength disturbances having a

small growth rate, so that the signal-to-noise ratio attains quite lowe values in this region. Moreover the fact that the beam size is comparable to the jet diameter will add further errors, as explained above. Large errors at very small wave numbers are explained instead by long-wave random disturbance during the measurement, like acoustic noise or unwanted vibrations that cannot be eliminated by the averaging procedure.

Figure 8 shows a comparison with experimental results from Donnelly and Glaberson (1965) obtained using the conventional photographic technique.

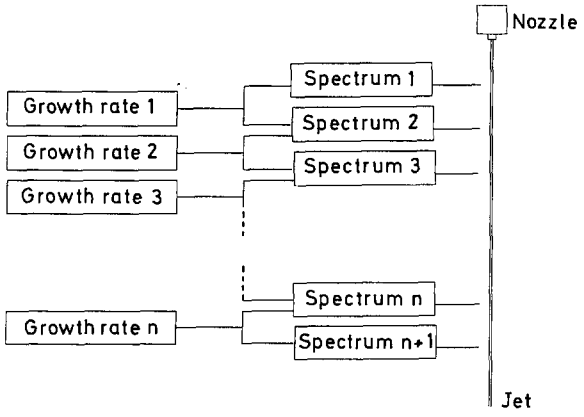

Fig. 6. Spectral comparison scheme

7 Concluding remarks

The proposed technique has given consistent results and comparison with existing experimental and theoretical results is satisfactory. Critical parameters seem to be the spacing and location of measurement points, and beam-jet relative diameter. The consistency checking procedure proposed here seems to work, although some subjectivity is involved. Results presented here show the capability of the technique but it should be pointed out that the present experimental situation was close to the limits of its applicability: use of smaller beam size or larger jet diameters is expected to greatly improve the performance. Moreover, the use of large samples in FFT analysis is expected to reduce variability en-

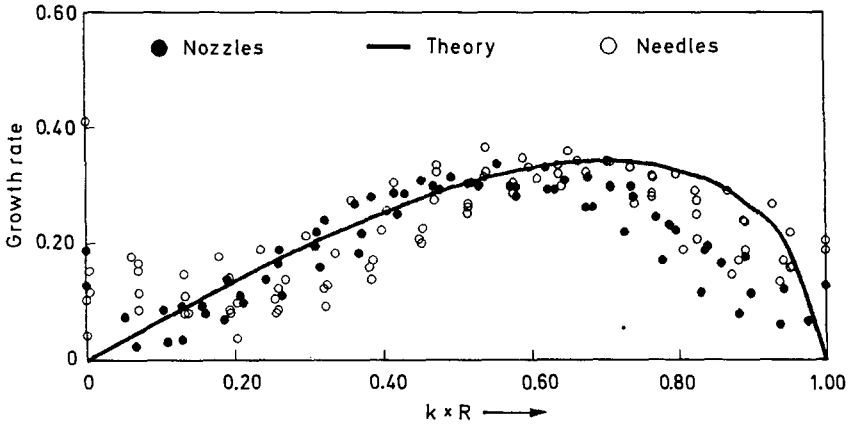

Fig. 7. Experimental results

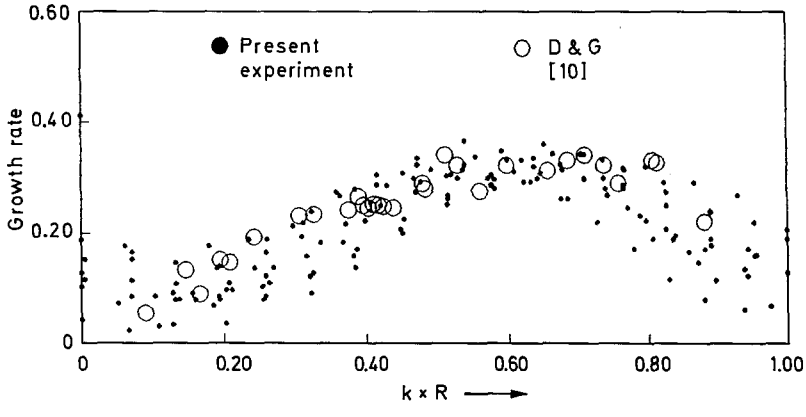

Fig. 8. Comparison between present experimental results and those from Donnelly and Glaberson (1965)

abling greater accuracy, even at the largest values of the perturbation wave number.

Acknowledgements

The authors would like to thank Mr. G. Brunello and Mr. P. Carmassi for their assistance during the experiments.

Appendix

Given the equation:

$$z_3 - z_0 = F(z_0) \tag{A1}$$

similar to Eq. (9) one would like to invert it and write:

$$z_0 - z_3 = G(z_3) \tag{A1b}$$

as in Eq. (11). If $F(x)$ is expanded in a Taylor's series one has:

$$F(z_3) = F(z_0) + F'(z_0)(z_3 - z_0) + F''(z_0)(z_3 - z_0)^2/2 + \ldots$$

Then, if: (A2)

$$|F'(z_0)(z_3 - z_0)| \ll |F(z_0)|$$
$$|F''(z_0)(z_3 - z_0)^2/2| \ll |F(z_0)|$$
$$\ldots\ldots\ldots\ldots\ldots\ldots\ldots$$
$$|F^{(n)}(z_0)(z_3 - z_0)^n/n!| \ll F(z_0)| \tag{A3}$$

one can put: $G(z_3) = -F(z_3)$.

Substituting (A1) into equations (A3) one obtains:

$$\left|\frac{F^{(n)}(F)^n}{n!}\right| \ll |F| \tag{A4}$$

where $F^{(k)}$ is the n-th derivative of the function $F(x)$ calculated in z_0; in the case of Eq. (9):

$$F(x) = 2(m_{12} - 1)[d - r(x) \cdot (m_{12} - 1)/m_{12}] \cdot r'(x) = D r'.$$

Let us suppose that $r(x)$ has the following form:

$$r(x) = R + a\, e^{ikx} \tag{A5}$$

i.e. the liquid column is a cylinder of radius R disturbed by a sinusoidal wave of amplitude "a" and wave number "k". By (A5) and (9) we get:

$$F^{(n)} = a \cdot k^{n+1}[D + (2^n - 1) \cdot a \cdot e^{ikx}] \cdot e^{ikx}$$
$$(F)^n = D^{n-1} \cdot a^{n-1} \cdot k^{n-1} \cdot (e^{ikx})^{n-1}$$

so that:

$$\left|\frac{F^{(n)}(F)^{n-1}}{n!}\right| = \frac{(a \cdot k^2 \cdot D)^n}{n!} \cdot \left[1 + \frac{a}{D}(2^n - 1)\right]. \tag{A6}$$

The first of the conditions (10) impose that $D \gg R$ and the second that $D \cdot a \cdot k^2 \ll 1$; the former then imposes that $a \ll D$ so that the term in square brackets in (A6) becomes important only for large n, and in that case

$$\left[1 + \frac{a}{D}(2^n - 1)\right] \approx 2^n a/D$$

so that for any value of n one can write (remembering the second of (10)):

$$\left|\frac{F^{(n)}(F)^{n-1}}{n!}\right| < \frac{(2a \cdot k^2 \cdot D)^n}{n!} \ll 1$$

and Eq. (11) holds.

The condition $D \cdot a \cdot k^2 \ll 1$ is much easily satisfied for small k, but k may became as large as $1/R$ and in that case the condition becomes:

$$\frac{D}{R} \cdot \frac{a}{R} \ll 1$$

showing that the linearization may be defective if the distance of the screen from the liquid column is too great or if the perturbation amplitude is too large.

References

Bohr, N. (1909): Determination of the surface tension of water by the method of jet vibration. Phil. Trans. Roy. Soc. A209, 281–317

Chandrasekhar, S. (1961): Hydrodynamic and hydromagnetic stability. Oxford, Clarendon Press

Donnelly, R. J.; Glaberson, W. (1965): Experiments on the capillarity instability of a liquid jet. Proc. Roy. Soc. A. Vol. 290

Levich, V. G. (1962): Physicochemical hydrodynamics. Prentice Hall

Levich, V. S.; Krylov, V. (1969): Surface, tension driven phenomena. Annual review of Fluid Mech., Vol. 1, p. 293

Rayleigh, Lord (1875): On the instability of jets. Proc. London Math. Soc. 10, 4–13

Sakai, T.; Sadakata, M.; Saito, M.; Matsushita, K. (1985): Studies on disintegration of liquid column between production of uniform size droplet by vibration method, ICLASS-85, VIIB (b)

Sleicher, C. A.; Sterling, A. M. (1975): The instability of capillary jets. J. Fluid Mech. Vol. 68, p. 477

Wang, D. P. (1968): Finite amplitude effect in the stability of a jet of circular cross-section. J. Fluid Mech. 34, 299–313, p. 25

Weber, C. (1931): On the Breakdown of a fluid jet. Z.A.M.P., Vol. 11, p. 136

Yuen, M. C. (1968): Nonlinear capillary instability of a liquid jet. J. Fluid Mech. 33, 151–163, p. 25

Received July 9, 1992